Microstructure Analysis of 4-Step Three-Dimensional Braided Composite

ZHENG Xi-tao, YE Tian-qi
(*Aircraft Department, Northwestern Polytechnic University, Xi'an 710072, China*)

Abstract: The yarn architecture of 3-D braided composites products by the four-step 1×1 braiding technique has been studied by means of a control volume method in conjunction with experimental investigation and a numerical method, respectively. An ellipse assumption for the cross-section of yarn was proposed in this analysis method with considering the yarn size and yarn-packing factor. Two types of local unit cell structures were identified for 4-step braided composites by considering the nature of the braiding processes and by observing the sample cross-sections. The relationship between the braiding procedure and the properties for 3-D braided structural shapes was established. This method provides the basis for analyzing stiffness and strength of 3-D braided composites.

Key words: composites; 3-D braided fabrics; unit cell; microstructure; packing factor
四步法三维编织复合材料细观结构分析. 郑锡涛, 叶天麒. 中国航空学报(英文版). 2003, 16(3): 142-150.

摘 要: 分别通过实验与控制体积方法系统地研究了采用四步法1×1方型编织工艺编织的预成形件的纱线结构。提出了纱线椭圆形横截面假设, 考虑了编织纱线的细度和编织纱线填充因子的影响。根据编织过程中携纱器的运动轨迹特点, 将预成形件划分为内部、表面和棱角3个不同的区域, 分别定义了不同的控制体积单元, 识别了预成形件的两种局部单胞模型, 分析了预成形件的纱线构造, 并导出了编织结构参数之间的关系。为编织复合材料的刚度、强度性能分析提供了充分的条件。

关键词: 复合材料; 三维编织; 细观结构; 单胞模型; 填充因子
文章编号: 1000-9361(2003)03-0142-09 中图分类号: TB332 文献标识码: A

The development of innovative fiber architecture and textile manufacturing technology has significantly expanded the potential of fiber-reinforced composites. Textile composites are being widely used in advanced structures in aviation, aerospace, automobile and marine industries[1]. An emerging area is textile composites reinforced with three-dimensional (3-D) preform. The integrated fiber network provides stiffness and strength in the thickness direction, thus reducing the potential of interlaminated failure, which often occurs in conventional laminated composites. Other distinct benefits of 3-D textile composites include the potential of automated processing from preform fabrication to matrix infiltration, and their near-net-shape forming capability, resulting in reduced machining, fastening, and scrap rate. In general, it is feasible to design textile structural composites with considerable flexibility in performance based upon a wide variety of preform geometries.

Textile composite technology by preforming is an application of textile processes to produce structured fabrics, known as preforms. The preform is then impregnated with a selected matrix material and consolidated into a permanent shape. Braiding with continuous fibers or yarns can place 3-D reinforcements in monocoque structural composites. Since the braiding procedure dictates the yarn structure in the preform and the yarn structure dictates the properties of the composite, designing

Received date: 2003-04-09; Revision received date: 2003-06-30
Foundation item: Aeronautical Science Foundation of China (99B23001)
Article URL: http://www.hkxb.net.cn/cja/2003/03/0142/

the braiding procedure to yield the desired structural shape that is endowed with the desired properties is an important element in textile composite technology[2].

The process-microstructure relationship of 3-D braided preforms was first studied by Li[3] *et al.*, and geometric relationships for the preform structure were established to predict the yarn orientation angle, braid dimensions, and yarn volume fraction. Wang and Wang[4] proposed an approach that attempted to bridge the relationship between the braiding procedure and the properties for 3-D braided structural shapes. The work of Du[5] *et al.* provided a detailed microstructure analysis of 2-step braided preforms, based upon a geometric model consisting of several types of unit cells. Byun and Chou[6] concluded that fiber architectures of braided preforms significantly influence the composite mechanical properties. Wu[7] developed a three-cells model. Chen[8] analyzed core/sheath structure of 4-step braided preforms.

In this investigation, an analysis method is presented to attempt to bridge the relationships between the braiding procedure and the properties for 3-D braided structural shapes. The developed method contains two major steps. The first step is to establish the general topology of the yarn structure based on the braiding procedure alone, the general topology being described in terms of some characterizing parameters. The second step is to relate the characterizing parameters to the final dimensions of the preform after consolidation. This then provides a full description of the yarn structure in the final shape.

The popular four-step 1 × 1 braiding procedure is used to demonstrate the successive developments. All of basic assumptions are proposed in Section 2. Determination of yarn structures in preforming states is contained in Section 3. An illustrative property modeling approach is described, where the yarn geometric relationship in the basic unit cells is derived. All results are expressed in explicit terms of the braiding parameters to demonstrate the direct link between the braiding parameters and the final shape properties in Section 4. In Sections 5 and 6, the yarn-packing factor and the fiber volume fraction in the composites are discussed, respectively. A set of summarizing remarks is contained in Section 7.

1 The Four-Step 1×1 Braiding Procedure

Several braiding methods are used to fabricate preforms. These are often classified by the kind of fabric they produce: 2-D or 3-D. The former is suitable for plate or thin-walled shape, while the latter is suitable for solid or thick-walled shapes. Many differing procedures exist for 3-D braiding, such as the two-step, four-step, the interlock process, *etc*[4]. The four-step 1 × 1 method will be adopted in this paper for the purpose of illustration only. Preforms of rectangular cross-section are analyzed to describe their yarn structure. Unit-cell-like substructures are identified in the interior, surfaces, and corners; and the total preform is represented by a structural composition of the unit cells.

A schematic set-up for the four-step 1 × 1 braiding procedure is shown in Fig. 1. The preform being braided is hung above the machine bed, on which yarn carriers are arranged in a prescribed

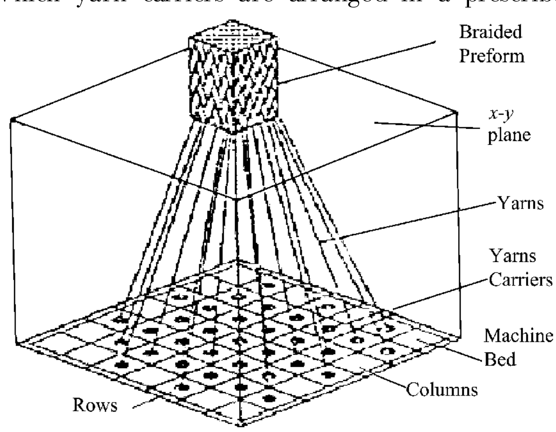

Fig. 1 Schematic of a 3-D braiding set-up

pattern. Braiding is realized through the movements of yarn carriers on the machine bed. Fig. 2 illustrates the carrier pattern and movements steps in one braiding cycle.

There are four carrier movement steps in one braiding cycle; in each carrier movement step, the carriers only move one position along either the column or the row directions[2]. Specifically, step-1 involves carrier motions in alternate rows and step-2 involves carrier motions in alternate columns; step-3 involves row motions that reverse those in step-1 and step-4 involves column motions

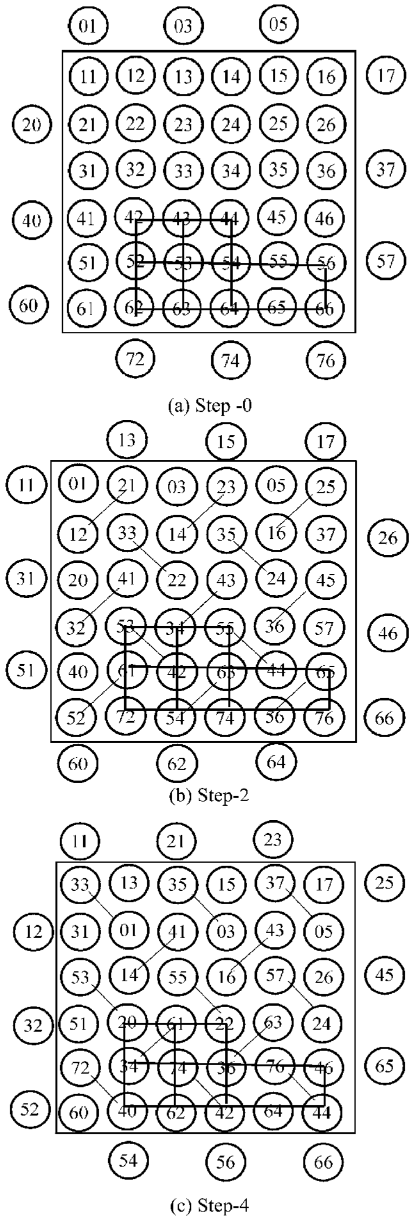

Fig. 2 4-step process

that reverse those in step-2. Note that the yarn carrier pattern after step-4 returns to the initial pattern, thus completing a cycle. After each cycle of braiding, the yarns are generally subjected to jamming action so the yarns are closely packed; and a finite length of the preform is realized, known as a pitch. Uniform jamming after each braiding cycle will result in a constant pitch along the length of the preform.

Clearly, the exact yarn carrier pattern dictates the cross-sectional shape of the preform. A rectangular pattern is commonly denoted by $[m \times n]$, m being the number of rows and n the number of columns of the yarn carriers on the machine bed. The set-up shown in Fig. 2 would furnish a $[6 \times 6]$ square cross-section. The actual size of the preform cross-section (also the pitch) depends on the yarn used and the condition of yarn jamming. It should also be noted that both the size and the shape of the preform may be changed during the matrix consolidation process.

The total yarns number N in the preform is

$$N = mn + m + n \qquad (1)$$

2 Basic Assumptions

Most of the previous studies on analytic characterization of 3-D textile composites have been limited to the preforms, and the proposed unit cells do not represent the entire structure in the case of 4-step braided composites. The cross-section of yarn round assumption is not suitable to the actual yarn in preform. In order to analyze actually the microstructure of 4-step braids, the following basic assumptions are proposed in this investigation:

(1) The cross-section perpendicular to the yarn length can be assumed as elliptical, and its major and minor axes lengths are respectively $2a$ and $2b$.

(2) Suppose the braiding procedure keeps relatively steady, at least in a specified length of braiding, to ensure consistent and uniform fabric structure.

(3) All yarns used in braiding the preform are the same fibers and have the same size and flexibility.

(4) All yarns used in braiding the preform have the same yarn-packing factor.

3 A Control-Volume Method for Yarn Topology

There have been studies devoted to describing the yarn network in 3-D braids. The general approach is to follow the braiding procedure and identify the yarn network in space. For the preform interior, a single repetitive unit cell is usually identified which is considered to represent the basic character of the preform yarn structure. On the boundary of the preform, unique yarn structures exist; this then necessitates separate yarn representation on the preform boundary.

Most of the studies, however, were aimed primarily at describing the yarn structures; the topological nature of yarn structures and the associated characteristics were not emphasized[6].

In this Section, a control volume method is outlined to describe the general topology in preforms braided by the four-step 1×1 procedure. The purpose is to demonstrate the association between the braiding procedure and the resulting yarn topology.

Follow the yarn carrier movements shown in Fig. 2 for one braiding cycle and trace the yarn paths in space. Instead of following all the carriers, a set of representative carriers will be selected. Fig. 2(a) shows the selected carriers (numbered 42-44, 52-54 and 62-64 at step-0); the subsequent movements of these carriers form a control space, or a control volume (CV). Thus, during the first two steps, carriers (42, 53) and (54, 63) exchange their respective position inside the CV; at the same time, carriers (43, 44, 52, 62, 64) move to position outside the CV. This forms four crisscrossing yarns inside the upper half of the CV. Similarly, during the next two steps, four crisscrossing yarns are formed in the lower half of the CV.

Essentially, the yarn trace in the CV discussed above characterizes the general topological character of the yarn structure in the preform interior. Specific characterization of the yarn topology will be explained in more detail below.

3.1 Basic unit cells of the interior

Assume that a uniform yarn jamming is applied after the braiding steps; the action will then straighten and reposition the yarns in the CV, as shown in Fig. 3. Specifically, the yarns in the front half of the CV form a sub-unit cell, denoted as sub-cell-A, and the yarns in the back half of the CV form a sub-unit cell, denoted as sub-cell-B. Yarn lines in sub-cell-A and sub-cell-B are shown

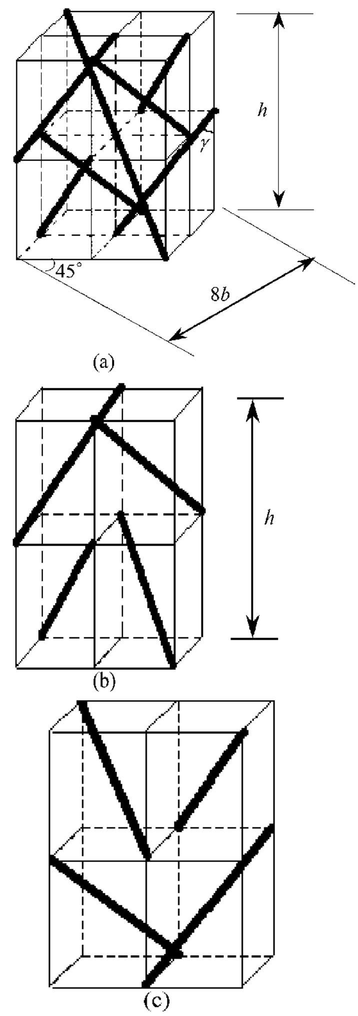

Fig.3 Interior unit cell structure in preform

in Fig. 3(b) and (c). Note that the jamming action defines yarn inclination angle γ in the unit cells and the pitch of the braid for one cycle, denoted by h.

The preform interior may be treated as a composition of the basic cells. It can be readily seen that the yarns in the interior unit cells form two families of flat plates which span the entire preform interior, as shown in Fig. 3(a). These plates intersect each other at right angles, and are orientated $\pm 45°$ with respect to the preform surfaces. Each of the flat plates is formed by two groups of crisscrossing yarns. These are, of course, the same crisscrossing yarns found in the unit cells.

For an interior unit cell, as shown in Fig. 3 (a), the width (W_i) and thickness (T_i) of the interior unit cell can be calculated from the assumption and geometric relationship of yarns

$$W_i = T_i = 4\sqrt{2}\,b \quad (2)$$

The braiding angle γ is

$$\tan\gamma = \frac{8b}{h} \quad (3)$$

The individual unit cells and the general topology of the interior as a while are now fully characterized by two free parameters; the braiding angle γ and the braiding pitch h. These two parameters remain free until the preform is consolidated into its final shape.

For an $[m \times n]$ braid preform, there are $(n-1)/2$ interior unit cells along the width direction of the preform and $(m-1)/2$ interior unit cells along the thickness direction.

3.2 Yarn topology on surface and the surface cell

To trace the yarns on the surface, it is convenient to select a 'control surface'. Referring to Fig. 2 at step-0 the vertical plane containing carriers (62-64) will be selected. Follow the carrier 62 for example; it exits the control surface from the interior at step-2 and re-enters at step-4. Upon yarn jamming, the yarns will be straightened (with a slight bend which is omitted here) and reposition themselves on the surface.

In actuality, yarns on the surface form a finite thickness layer, depending on the size of the yarn used. A basic cell on the surface may be defined, as shown in Fig. 4. The yarn topology in the cell is characterized by the angle β and the pitch h. The

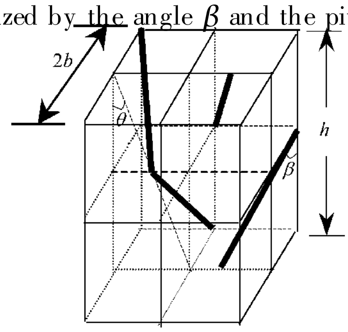

Fig. 4 Surface unit cell structure in preform

yarns lying in the surface incline with the braiding axis at the angle θ.

Similarly, for a surface unit cell (see Fig. 4), the width (W_s) of the surface unit cell can be calculated from the assumption and geometric relationship of yarns

$$W_s = 4\sqrt{2}\,b \quad (4)$$

The thickness (T_s) of the surface unit cell is

$$T_s = 2b \quad (5)$$

In theory, yarns in the surface unit cell should be space curves. In order to simplify the model, straight lines were used to replace the curve yarns. The surface-braiding angle β is defined as the angle between yarn and braiding axis (see Fig. 4). Thus

$$\tan\beta = \frac{2\sqrt{3}\,b}{h} \quad (6)$$

The surface yarn inclination angle θ is defined as the angle between yarn projection on the surface and braiding axis direction.

$$\tan\theta = \frac{2\sqrt{2}\,b}{h} \quad (7)$$

From the geometry shown in Fig. 4, the surface yarn inclination angle θ is readily related to the braiding angle γ of the interior. Thus,

$$\tan\theta = \frac{W_s}{2h} = \frac{\sqrt{2}}{4}\tan\gamma \quad (8)$$

The surface look is relevant for the fact that only the surface yarn inclination angle θ and the braiding pitch h can be readily measured with precision. Since it is generally difficult to measure the interior braiding angle γ, Eq. (8) can be used to calculate γ by knowing θ.

For an $[m \times n]$ yarn arrangement, there are $(n-1)/2$ surface unit cells along the width direction of the preform and $(m-1)/2$ surface unit cells along the thickness direction. It can also be shown that in preforms of a rectangular cross-section, the same surface cell is found on surfaces of opposing sides; the mirror image of that surface cell is found on surfaces of the other pair of opposing sides.

3.3 Cell composition of preform

At this point, the topology of the entire preform has been established, along with the various unit cells identified; all are expressed in terms of the free parameters, the braiding angle γ and the pitch length h. The values of the latter can be measured, given the final dimensions of the preform; so the yarn structure in the preform is fully described. Furthermore, the entire preform is a structural composition of the interior cells (A and B), surface cells, and corner cells. The exact cell composition is easily determined by the carrier arrangement on the machine bed. In the case of a rectangular solid cross-section, for instance, the integer values in $[m \times n]$ determine the exact cell composition.

In a micro-structural analysis, a 3-D braided preform exhibiting a core/sheath structure can be divided into three regions, *i.e.* the interior, surface, and corner, each of which has unique yarn architecture, as shown in Fig. 5.

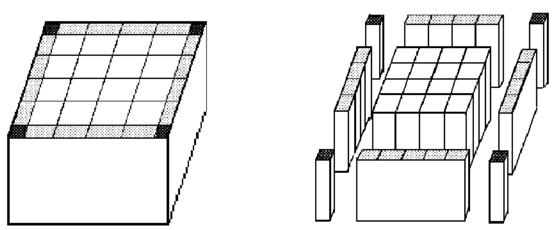

Fig. 5　Core/sheath structure of preform

For an $[m \times n]$ braid, the volume proportion of each region to the entire structure is deduced as follows

$$V_i = \frac{(m-1)(n-1)}{mn + (\sqrt{2}-1)m + (\sqrt{2}-1)n - 2\sqrt{2} + 3}$$

$$V_s = \frac{\sqrt{2}(m+n-2)}{mn + (\sqrt{2}-1)m + (\sqrt{2}-1)n - 2\sqrt{2} + 3}$$

$$V_c = \frac{2}{mn + (\sqrt{2}-1)m + (\sqrt{2}-1)n - 2\sqrt{2} + 3} \qquad (9)$$

where V_i, V_s, V_c are, respectively, the volume proportion of interior, surface, corner regions to the whole structure in the preform.

From Eq. (9), the volume proportion of surface region to whole structure in the preform depends upon the numbers of yarns, m and n. When the numbers of yarns, m or n, tend to a minor number, the volume proportion of the surface region is over 30% of the whole structure in the preform. So the effect of the surface region on the entire structure cannot be neglected.

Table 1 shows the calculation obtained by Eq. (9) for the specimens used in this study. It is clear that the volume proportion of corner region to whole structure is smaller than 3%, so its influence on the whole structure can be ignored and it is replaced by the surface region in calculating. Moreover, the volume proportion of surface region to whole structure changed to be

$$V_s = 1 - V_i \qquad (10)$$

The same simplified method to deal with the boundary region of 3-D preforms has been used by Chen[8].

Table 1　The volume proportion of each region to whole structure in the preform

Specimens	Yarns	Volume proportion of each region		
Number	$m \times n$	Interior/%	Surface/%	Corner/%
CT2045	4×23	63.86	34.21	1.94
CT4045	3×22	54.88	42.50	2.61
CT2055	5×25	69.77	28.78	1.45
CT4055	4×23	63.86	34.21	1.94

4　Composite Geometry

Once the dimensional parameters of yarns are determined, the geometric characteristics of the composite can be identified based upon the unit cell approach. From Fig. 5, the width (W) and the thickness (T) of composite can be expressed in terms of the number of yarns and their sizes

$$W = 2 \times [\sqrt{2}(n-1) + 2]b \qquad (11)$$

$$T = 2 \times [\sqrt{2}(m-1) + 2]b \qquad (12)$$

Put Eq. (3) into Eqs. (11) and (12), the pitch length h can be expressed as

$$h = \frac{8b}{\tan\gamma} = \frac{4W}{[\sqrt{2}(n-1) + 2]\tan\gamma} \qquad (13)$$

or

$$h = \frac{8b}{\tan\gamma} = \frac{4T}{[\sqrt{2}(m-1) + 2]\tan\gamma} \qquad (14)$$

Eqs. (13) and (14) state clearly the pitch length decreases with the braiding angle and numbers of yarns increasing as the dimension of the preform keeps constant.

Table 2 shows the measured and predicted geometric parameters of composite specimens. The measurement data are gained from the average values of five specimens. The calculation was obtained by Eqs. (12) and (13). The comparison is quite satisfactory. Some discrepancies are found in the thickness for the specimens with larger braid angles (denoted by 40 in the specimens numbers).

Table 2 Predication and test results for thickness of preform and braiding pitch length

Specimens number	Thickness (mm)		Pitch length (mm)	
	Measured	Predicted	Measured	Predicted
CT2045	4.99	4.69	11.73	11.38
CT4045	4.97	4.90	3.69	3.87
CT2055	5.16	5.31	10.87	10.94
CT4055	5.46	4.72	3.80	3.92
GT2045	5.01	4.70	12.89	13.57
GT4045	5.38	4.91	3.20	3.42
GT2055	5.31	5.33	11.62	11.69
GT4055	5.51	4.71	3.38	3.55
CB2045	5.27	4.69	9.57	9.13
CB4045	4.88	4.93	3.40	3.50
CB2055	5.03	5.29	11.18	11.70
CB4055	5.47	4.72	3.68	3.79

5 Fiber Packing Fraction

Fiber packing fraction k is the fiber volume fraction in a yarn. It is defined as follow

$$k = \frac{\pi D_y^2}{4\Omega} = \frac{D_y^2}{4ab} \tag{15}$$

where $D_y = \sqrt{4\lambda/\pi\rho}$ is the equivalent diameter (mm) of the yarn; λ and ρ are, respectively, the linear density (kg/m) of yarns and fiber density (kg/m^3).

For fiber yarns, the fiber packing fraction changes complexly during the braiding procedure. The fiber packing fraction changes as redistribution of bearing force among yarns. At this point, the change of the fiber packing fraction will be ignored during the braiding procedure and the fiber packing fraction will be only considered in the final preform.

Based upon the assumptions, put Eqs. (13) and (14) into Eq. (15), and the fiber packing fraction can be expressed as follows

$$k = \frac{D_y^2[\sqrt{2}(n-1)+2]^2}{\sqrt{3}W^2\cos\gamma} \tag{16}$$

or

$$k = \frac{D_y^2[\sqrt{2}(m-1)+2]^2}{\sqrt{3}T^2\cos\gamma} \tag{17}$$

From these equations, it is clear that the fiber packing factor increases with braided angle increasing and decreases with dimension of preform increasing when the number of braiding yarns [$m \times n$] keeps constant. During the braiding procedure, the fiber-packing factor has two critical states: one is the initial state of yarn; the other is the crowded state when the fibers in the yarn are arranged in hexagon. At this time, the fiber-packing factor reaches its maximum value, $k = \pi/(2\sqrt{3}) \approx 0.9069$.

6 Fiber Volume Fraction

Since the yarn cross-sectional area and orientation angle have been obtained in Section 3, the yarn volume in the preforms can be readily determined. Considering the actual length and cross-section of a yarn, the fiber content in a unit cell can be obtained by multiplying yarn content by fiber packing fraction.

6.1 Fiber volume fraction in interior and boundary

The volume of an interior unit cell (see Fig. 3(a)) is

$$U_i = W_i T_i h = \frac{h^3\tan^2\gamma}{2} \tag{18}$$

The total yarn volume in the interior unit cell is

$$Y_i = \frac{4\pi abh}{\cos\gamma} \tag{19}$$

The fiber volume fraction in the interior unit cell can be obtained by multiplying yarn volume of interior by fiber packing fraction and be expressed as

$$V_{if} = \frac{Y_i}{U_i}k = \frac{\pi\sqrt{3}}{8}k \tag{20}$$

The volume of a surface unit cell (see Fig. 4) is

$$U_s = W_s T_s h = \frac{\sqrt{2}}{8}h^3\tan^2\gamma \tag{21}$$

The total yarn volume in the surface unit cell is

$$Y_s = 4\pi ab \frac{h}{2\cos\beta} \frac{2\pi abh}{\cos\beta} \quad (22)$$

The fiber volume fraction in the surface unit cell can be obtained by multiplying yarn volume by fiber packing fraction and expressed as

$$V_{sf} = \frac{Y_s}{U_s}k = \frac{\sqrt{6}\,\pi\cos\gamma}{8\cos\beta} \quad (23)$$

6.2 Total fiber volume fraction

The total fiber volume fraction of the composite, V_f, is the sum of multiplying the fiber volume fraction by volume proportion in every region. Thus

$$V_f = V_i V_{if} + V_s V_{sf} \quad (24)$$

where V_i, V_s are, respectively, the volume proportion of interior, surface regions to entire structure in the preform, obtained from Eqs. (9) and (10). V_{if}, V_{sf} are, respectively, the fiber volume fraction of interior, surface regions, obtained from Eqs. (20) and (23).

The total fiber volume fraction in the preform varies with the number of braiding yarns [$m \times n$], braiding angle and fiber packing fraction. The variation of yarn number [$m \times n$] results in changing the volume proportion of each region to whole structure in the preform. With increasing the number of m and n, the volume proportion of the surface region will reduce; the total fiber volume fraction will also reduce and tend to the value of fiber volume fraction of interior. Otherwise, the total fiber volume fraction will increase with the fiber packing fraction. When the number of m and n keeps constant, the increasing of the braiding angle results in increasing of the fiber packing fraction and total fiber volume fraction.

Table 3 gives the comparison of the measured and predicted fiber volume fraction and the surface yarn inclination angle of composite specimens. The measurement data are gained from the average values of five specimens. The calculation was obtained by Eqs. (24), (16) and (7), respectively. The measured and predicted data of the fiber volume fraction and the surface yarn inclination angles are in good agreement. At the same time, it is found that the yarn-packing factor is bigger for the specimen with a larger braiding angle as the different specimens have the same fiber volume fraction.

Table 3 Predication and test results for fiber volume fraction in the preforms

Specimens number	Fiber volume fraction (%)			Fiber packing factor	Surface braid angle (°)		
	Measured	Predicted	Error (%)		Measured	Predicted	Error (%)
CT2045	44.23	47.23	6.79	0.613	9.94	10.75	8.18
CT4045	43.65	50.65	16.05	0.696	29.56	29.90	1.17
CT2055	56.76	54.31	-4.30	0.716	9.82	10.22	4.10
CT4055	48.17	52.80	9.61	0.724	27.22	28.66	5.30
GT2045	52.84	48.96	-7.34	0.605	9.28	9.18	-1.12
GT4045	48.77	53.41	9.51	0.708	31.02	33.21	7.07
GT2055	63.44	55.92	-11.85	0.709	9.26	9.57	3.31
GT4055	60.61	58.27	-3.86	0.786	31.96	31.19	-2.40
CB2045	42.82	47.58	11.13	0.617	12.73	13.11	2.98
CB4045	45.20	52.13	15.33	0.726	32.80	32.57	-0.69
CB2055	56.29	54.69	-2.84	0.721	10.13	9.50	-6.21
CB4055	48.43	53.33	10.11	0.735	28.27	29.43	4.10

7 Conclusions

The results of this systematic analysis for establishing the process-microstructure relationship of 4-step braided composites are summarized as follows.

(1) An analysis method is presented which describes the yarn structures in 3-D braided preforms. By tracing the yarn lines in space during the braiding cycle, the general topology of the yarn structure can be analytically established, which depends solely on the braiding method. From the general topology, basic unit cells in the interior and on the boundary are identified and the preform as a whole is treated as a structural composition of the basic cells.

(2) From the overall yarn structure in the preform, two types of unit cell structures were

identified for 4-step braided composites in the preform interior and on its boundary. It should be noted that substructuring of a 3-D preform in terms of small unit cells is essential for property characterization. A treatment of this subject[9] has been reported elsewhere.

(3) The preform interior consists of two types of sub-cells. On the boundary of the preform, the same surface cell is found on surfaces of opposing sides; the mirror image of that surface cell is found on surfaces of the other pair of opposing sides.

(4) The pitch length decreases with the braiding angle and numbers of yarns increasing as the dimension of the preform keeps constant.

(5) The fiber-packing factor increases with the braided angle increasing and decreases with dimension of preform increasing when the number of braiding yarns [$m \times n$] keeps constant. During the braiding procedure, the fiber-packing factor presents two critical states: one is the initial state of yarn; the other is the crowded state when the fibers in the yarn are arranged in hexagon. At this time, the fiber-packing factor reaches its maximum value, $k \approx 0.9069$.

(6) The total fiber volume fraction in preform varies with the number of braiding yarns [$m \times n$], braiding angle and fiber packing fraction. The variation of yarn number [$m \times n$] results in changing the volume proportion of each region to whole structure in the preform. With increasing the number of m and n, the volume proportion of the surface region will reduce; the total fiber volume fraction will also reduce and tend to the value of fiber volume fraction of interior. Otherwise, the total fiber volume fraction will increase with the fiber packing fraction. When the number of m and n keeps constant, the increasing of braiding angle results in increasing of the fiber packing fraction and total fiber volume fraction.

Finally, it is mentioned that the method presented in this paper can be also applied to analyze 3-D five directions, six directions and seven directions braiding preforms.

References

[1] 黄故. 现代纺织复合材料[M]. 北京: 中国纺织出版社, 2000.
Huang G. Modern textile composites [M]. Beijing: Chinese Textile Press, 2000.

[2] Wang Y Q, Wang A S D. On the topological yarn structure of 3-D rectangular and tubular braided preforms[J]. Composites Science and Technology, 1994, 51(2): 575-586.

[3] Li W, Hammad M, El-Shiekh A. Structural analysis of 3-D braided preforms for composites [J]. J Text Inst, 1990, 81: 491-514.

[4] Wang Y Q, Wang A S D. Microstructure/property relationships in three-dimensionally braided fiber composites[J]. Composites Science and Technology, 1995, 53(2): 213-222.

[5] Du G W, Popper P, Chou T W. Analysis of 3-D textile preforms for multidirectional reinforcement of composites [J]. J Mater Sci, 1991, 26: 3438-3448.

[6] Byun J H, Chou T W. Process-microstructure relationships of 2-step and 4-step braided composites [J]. Composites Science and Technology, 1996, 56: 235-251.

[7] Wu D L. Three-cell model and 5D braided structural composites [J]. Composites Science and Technology, 1996, 56: 225-233.

[8] 陈利. 三维编织复合材料的细观结构及其弹性性能分析[D]. 天津: 天津纺织工学院. 1998.
Chen L. Microstructure and elastic properties of 3D braided composites [D]. Tianjing: Tianjing Textile College. 1998.

[9] 郑锡涛, 陈利, 李家禄, 等. 三维编织复合材料中纱线的运动规律及细观模型[J]. 机械科学与技术, 2001, 20(增刊): 57-61.
(Zheng X T, Chen L, Li J L, *et al*. The movement rule of yarn and micro-structural model in 3-D braided composites [J]. Mechanical Science and Technology, 2001, 20(Sup.): 57-61.

Biographies:

ZHENG Xi-tao Born in 1964, he is a Ph D candidate of Northwestern Polytechnic University. He received B. S. from NPU in 1986, and then worked in Aircraft Strength Research Institute. From 1993 to 1994, he did cooperative research work in DLR of Germany. He has published over 40 scientific papers in various periodicals. Tel: (029) 8213623-8132, E-mail: ademcock@pub.xaonline.com

YE Tian-qi Born in 1933, Ph. D, Professor of Computational Mechanics and Aircraft Structures. Interested field: Adaptive methods in FEM and BEM, Parallel processing in FEM, Application of wavelet analysis in solid mechanics, Dynamic contact, Fluid-solid interaction, Nonlinear analysis of shells, Heat transfer in spacecraft structures.